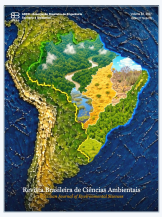
rbciamb



Volume 62
2027

Received
02/04/2026

Accepted
09/28/2026

DOI
10.67790/rbciamb.027.2936

Affiliation

[1]Federal University of Amazonas (UFAM), Humaitá (AM), Brazil.

[2]Federal University of Pará (UFPA), Belém (PA), Brazil.

Corresponding author

Anderson de Souza Carneiro
E-mail: andersondsc17@gmail.com

This is an open access article distributed under the terms of the Creative Commons license.

Monitoring of $PM_{2.5}$ and PM_{10} particulate matter concentrations in an urban area of Southern Amazonas, Brazil

Monitoramento das concentrações de materiais particulados $MP_{2.5}$ e MP_{10} em área urbana no Sul do Amazonas, Brasil

Anderson de Souza Carneiro[1], Jorge Almeida de Menezes[1], Carlos Barbosa Pessoa[1], Amazonino Lemos de Castro[1], Rafael da Silva Palácios[2]

Abstract

Humaitá, located in Southern Amazonas, has been increasingly affected by environmental pressures associated with agricultural frontier expansion, deforestation, and the intensification of biomass burning. This study analyzed the seasonal variability of $PM_{2.5}$ and PM_{10} between 2023 and 2024 using data from the first automatic air quality monitoring station installed in Southern Amazonas. The approach integrated continuous air quality monitoring, backward air-mass trajectory modeling, and logistic regression to identify quantitative thresholds for exceedance of air quality standards. The results revealed marked seasonality, with particulate matter (PM) concentrations below 10 μg m^{-3} during the rainy season, associated with high precipitation (>300 mm). In contrast, substantial increases occurred between June and September, with accumulated precipitation below 15 mm during the June–August quarter, while fire hotspots intensified throughout the Southern Amazon region. At the state level, Humaitá accounted for approximately 5.5% of all fire hotspots recorded by INPE in Amazonas during 2024. In 2024, the number of fire hotspots was 31% higher than that recorded in 2023, accompanied by increased particulate matter concentrations. Peak concentrations were observed in September 2024, reaching 172.3 μg m^{-3} for $PM_{2.5}$ and 176.0 μg m^{-3} for PM_{10}. A total of 68 and 64 days exceeded the daily $PM_{2.5}$ standard of 15 μg m^{-3} in 2023 and 2024, respectively, with 2024 characterized by more severe episodes classified as "Very Poor (*Muito Ruim*)" and "Very Bad (*Péssima*)" according to the Brazilian Air Quality Index (AQI). Threshold analysis indicated a 50% probability of exceeding the daily standard at 85 fire hotspots day^{-1} and an 80% probability at 134 fire hotspots day^{-1}. Correlations among $PM_{2.5}$, PM_{10}, fire hotspots, and meteorological variables confirmed the strong influence of biomass burning on air quality degradation in the region.

Keywords Seasonal variability · Air quality · Biomass burning · Meteorological variability · Atmospheric pollution

Resumo

Humaitá, no Sul do Amazonas, enfrenta crescentes pressões ambientais associadas à expansão da fronteira agrícola, ao desmatamento e à intensificação das queimadas. Este estudo analisou a variabilidade sazonal do $MP_{2.5}$ e MP_{10} entre 2023 e 2024, utilizando dados da primeira estação automática de monitoramento da região Sul do Amazonas. A abordagem integrou monitoramento contínuo, modelagem de trajetórias atmosféricas e regressão logística para identificar limiares quantitativos de excedência dos padrões de qualidade do ar. Os resultados evidenciaram forte sazonalidade, com concentrações inferiores a 10 μg m^{-3} no período chuvoso, associadas à elevada precipitação (>300 mm). Em contraste, aumentos expressivos ocorreram entre junho e setembro, quando a precipitação média foi inferior a 5 mm $mês^{-1}$ e os focos de queimadas se intensificaram em toda a região sul amazônica. No contexto estadual, Humaitá destacou-se em 2024 ao responder por cerca de 5,5% dos focos de queimadas registrados pelo INPE no Amazonas. Em 2024, o número de focos de queimadas foi 31% superior ao observado em 2023, associado ao aumento das concentrações de material particulado. Os maiores valores ocorreram em setembro de 2024, com concentrações de 172,3 μg m^{-3} para $MP_{2.5}$ e 176,0 μg m^{-3} para MP_{10}. Foram registrados 68 e 64 dias acima do limite diário de 15 μg m^{-3} para $MP_{2.5}$ em 2023 e 2024, respectivamente, sendo 2024 marcado por episódios mais severos classificados como "Muito Ruim" e "Péssima". A análise de limiar indicou probabilidade de 50% de excedência do limite diário com 85 focos dia^{-1} e 80% com 134 focos dia^{-1}. As correlações entre $MP_{2.5}$, MP_{10}, focos de queimadas e variáveis meteorológicas evidenciaram a influência da queima de biomassa na degradação da qualidade do ar na região.

Palavras-chave Variabilidade sazonal · Qualidade do ar · Queima de biomassa · Variabilidade meteorológica · Poluição atmosférica

1 Introduction

Atmospheric pollution constitutes one of the major environmental and public health challenges of the 21st century, especially in tropical regions undergoing intense socio-environmental transformation, such as the Brazilian Amazon. Among the main atmospheric pollutants, particulate matter (PM) stands out, classified according to aerodynamic diameter into fine particles ($PM_{2.5}$; < 2.5 μm) and inhalable particles (PM_{10}; < 10 μm) (WHO, 2021).

$PM_{2.5}$ particles are considered critical to health because of their ability to reach the deep portions of the respiratory system, reaching the lung alveoli and potentially crossing the alveolar epithelial barrier, entering the bloodstream, and triggering systemic effects in several organs, mainly the cardiovascular system (Yamagishi et al., 2020; Feng et al., 2024). Such effects manifest in the short and long term, especially in urban populations exposed to high concentrations of atmospheric pollutants (Santos et al., 2021).

In Brazil, the main sources of atmospheric PM in urban areas include vehicular emissions, industrial activities, resuspension of road dust, and biomass burning, which are responsible for critical episodes of air quality degradation, especially during dry periods with high atmospheric stability (Pacheco et al., 2017; Pereira et al., 2025). In the Brazilian Amazon, atmospheric particle emissions are directly associated with deforestation, conversion of forest to livestock activities, use of fire in family farming, and agribusiness expansion (Fearnside, 2022).

The impacts of forest fires extend beyond the Amazon deforestation arc, affecting distant urban centers through the long-range transport of aerosols. Amazonian municipalities such as Humaitá, located close to the emitting sources, are among the most affected. During the extreme fire event associated with the severe 2023–2024 El Niño drought, aerosols from the Amazon reached Southeast and Southern Brazil, driven by the South American Low-Level Jet (SALLJ), which transports emissions to subtropical regions (Marengo et al., 2024; Forgioni et al., 2025).

Given the increasing frequency of these episodes, continuous air quality monitoring becomes essential for the early detection of pollution peaks and the mitigation of health impacts (Palmisani et al., 2021). Brazilian monitoring infrastructure remains uneven, concentrated in the Southeast region, with low coverage in the Amazon (Vormittag et al., 2021; IEMA, 2024). According to the Energy and Environment Institute (IEMA), only 12 of the 26 Brazilian states have some type of air quality monitoring, evidencing the limited national coverage and the need to expand atmospheric observation networks.

This gap compromises the representativeness of the data, especially in critical areas such as the Amazon, which lack systematic observation networks (Andreão and Almeida Albuquerque, 2020; Vormittag et al., 2021). In this context, this study integrates continuous surface air quality data obtained from the first automatic monitoring station installed in Southern Amazonas state with backward trajectory modeling, allowing the simultaneous investigation of the influence of local emissions and of the regional transport of atmospheric pollutants, overcoming the limitations of analyses based exclusively on fire hotspot counts, which do not distinguish scenarios with different atmospheric exposure potentials.

Thus, this study aims to evaluate the temporal variability of $PM_{2.5}$ and PM_{10} concentrations in the municipality of Humaitá between 2023 and 2024, to analyze the influence of atmospheric transport on the episodes of highest PM concentration through the analysis of backward air mass trajectories obtained with the HYSPLIT model, and to compare the observed levels with the criteria of the Air Quality Index (AQI) established by CONAMA Resolution No. 506/2024 (CONAMA, 2024). The study further establishes a logistic regression model to estimate the probability of exceeding $PM_{2.5}$ concentrations as a function of the number of fire hotspots, identifying operational thresholds that support early warning systems and air quality management strategies based on fire dynamics.

2 Methodology

2.1 Study area

The study area corresponds to the urban zone of the municipality of Humaitá, located in the Southern mesoregion of Amazonas state, Brazil (Figure 1). Its territorial extension covers approximately 33,111.129 km^2, with an estimated population of 57,473 inhabitants (IBGE, 2022). The municipality is part of the Amazon deforestation arc, a region marked by agrarian expansion and the occurrence of fires.

According to the Köppen classification, the municipality has a tropical monsoon climate (Am), characterized by a rainy season between November and April, with annual precipitation of 2,500 mm and monthly average above 300 mm, and a dry season between June and September, with monthly means close to 50 mm; May and October are transition months. The mean annual temperature ranges between 25 °C and 27 °C, with maxima up to 36 °C in the hottest months and occasional minima of 17 °C during cold-spell episodes. Relative humidity remains between 85% and 90% in the rainy season and may drop to values close to 50% in the dry season (Martins et al., 2023; Pereira and Querino, 2025).

The monitoring station was installed on the premises of the Centro Educacional de Tempo Integral (CETI) — Full-Time Educational Center — identified by the red point in Figure 1, at coordinates 07°31′32.65″S; 63°02′28.04″W. The installation followed the guidelines of the Technical Guide for Air Quality Monitoring and Assessment (Brasil, 2020) and the technical criteria established by the EPA (2017).

The study region has no local atmospheric emission inventory, limiting the direct quantification of emitting sources. The monitoring point is under the influence of different potential sources, with biomass burning prevailing as the main source of PM in the region, in addition to vehicular emissions associated with heavy vehicle traffic and dust resuspension on urban roads.

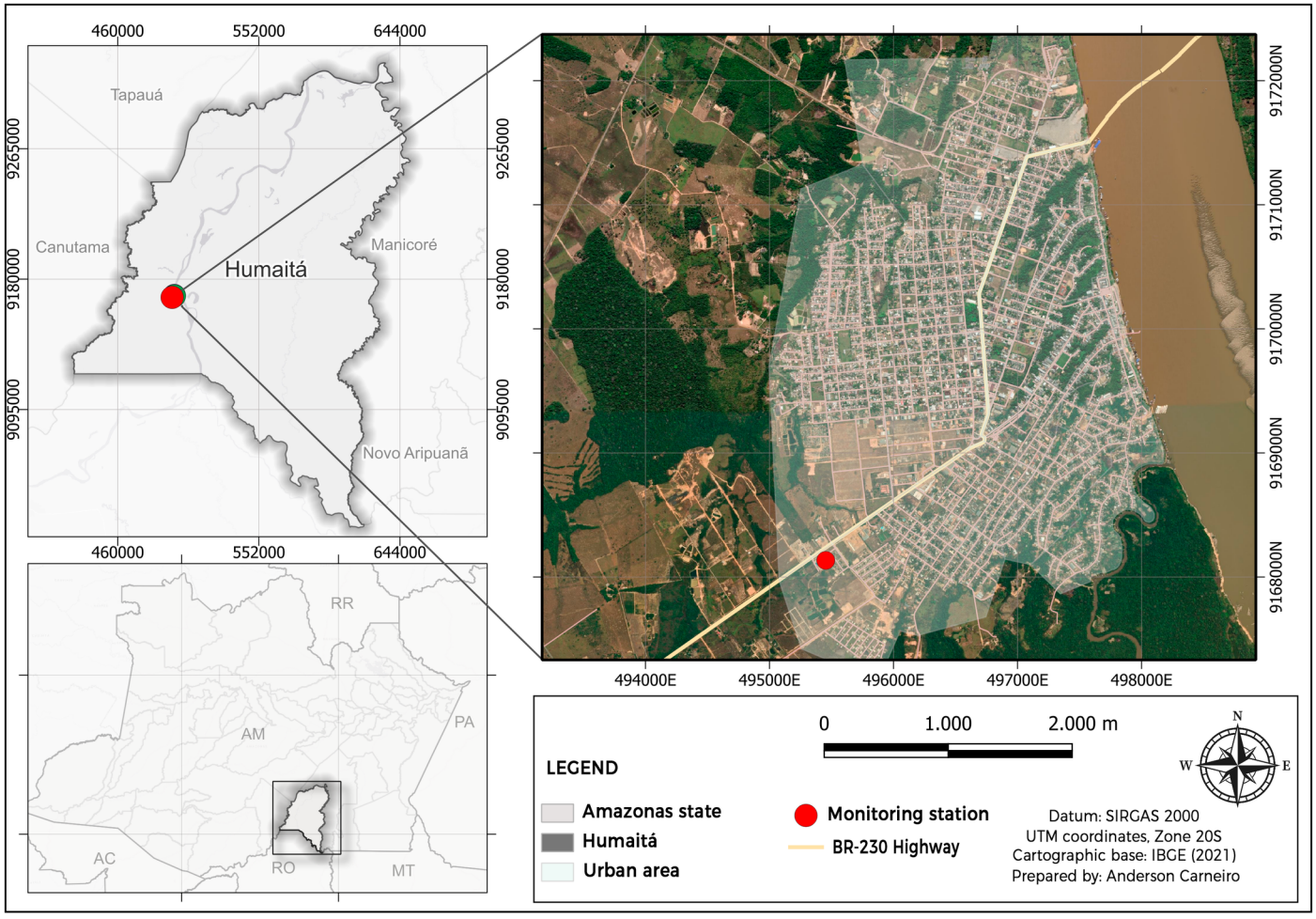


Figure 1. Location of the urban area of the municipality of Humaitá-AM and of the automatic air quality monitoring station

2.2 Data collection

The automatic monitoring station, an ECOPM monitor from the ECOPX line, is equipped with an optical particle counter (OPC) based on the principle of optical light scattering (Jang et al., 2022). This monitor records $PM_{2.5}$ and PM_{10} concentrations with a measurement range of 0–2,000 μg m^{-3}, a sensitivity of 0.1 μg m^{-3}, and a sampling flow rate between 0.05 and 0.35 L min^{-1}. Measurements were performed continuously with a temporal resolution of 60 seconds. The monitor is equipped with air temperature (T) and relative humidity (RH) sensors.

Although they do not correspond to the Federal Reference Method (FRM/EPA), OPC-based methods are widely used for $PM_{2.5}$ monitoring during critical pollution episodes and are recognized by the EPA as suitable alternatives for atmospheric applications, provided that they are properly sited, installed, configured, operated, and maintained (EPA, 2022). However, OPC sensors may present uncertainties under high relative humidity because of the hygroscopic growth of aerosols (Jayaratne et al., 2018).

The monitoring campaign was conducted continuously between January 2023 and November 2024. Fire hotspots were obtained from the Queimadas/INPE Program, integrating the MODIS, VIIRS, and GOES-16 sensors (INPE, 2024). Accumulated precipitation data were obtained from the ERA5-Land reanalysis (ECMWF, ~9 km) (Hersbach et al., 2020). Backward air mass trajectories for August and September of each year were generated with the HYSPLIT model (NOAA/GDAS, 1°) (Stein et al., 2015).

2.3 Statistical analysis of the data

The analyses were conducted in Python using the NumPy, Pandas, Matplotlib, and SciPy libraries. The data were analyzed on two temporal scales: (i) daily and (ii) monthly averages, in addition to descriptive statistical analyses. Daily averages were compared with the standards established by CONAMA Resolution No. 506/2024, which defines limits of 15 μg m^{-3} for $PM_{2.5}$ and 45 μg m^{-3} for PM_{10} for 24-hour averages. To estimate the impact of the concentrations on atmospheric pollution, the AQI was calculated according to Equation (1).

$$AQI = I_{ini} + \frac{I_{fin} - I_{ini}}{C_{fin} - C_{ini}} \times (C - C_{ini}) \quad (1)$$

where: AQI = Air Quality Index; Iini = index value corresponding to the initial concentration of the range; Ifin = index value corresponding to the final concentration of the range; Cini = initial concentration of

the range in which the measured concentration falls; Cfin = final concentration of the range; C = measured concentration of the pollutant.

To investigate the relationships between $PM_{2.5}$ and PM_{10} concentrations and the meteorological variables and fire hotspots, the Pearson correlation coefficient (r) was applied, according to Equation (2), based on combined monthly averages (n = 23). The significance level adopted was $\alpha = 0.05$.

$$r = \frac{\Sigma(x_i - \bar{x})(y_i - \bar{y})}{\sqrt{\Sigma(x_i - \bar{x})^2 \times \Sigma(y_i - \bar{y})^2}} \quad (2)$$

The critical threshold analysis was conducted by means of multivariate binary logistic regression, including as independent variables the daily number of fire hotspots, air temperature (T), and relative humidity (RH), to estimate the probability of exceeding the daily $PM_{2.5}$ limit of 15 μg m^{-3} (CONAMA, 2024), following Rincon et al. (2022). The model was evaluated using the ROC curve (AUC-ROC) and the Kruskal–Wallis test for comparing concentrations among fire intensity classes. The adopted logistic model is given by Equation (3):

$$P_i = \frac{1}{1 + e^{-(\beta_0 + \beta_1 F_i + \beta_2 T_i + \beta_3 U_i)}} \quad (3)$$

where P_i is the probability of exceedance on day i; F_i represents the number of fire hotspots; T_i the air temperature; and U_i the air relative humidity. The term β_0 corresponds to the model intercept, while β_1, β_2, and β_3 represent the coefficients of the explanatory variables. The fit was performed by the maximum likelihood method, while the discriminatory performance was evaluated by the area under the ROC curve (AUC-ROC), used to assess the model's ability to distinguish exceedance events of the daily $PM_{2.5}$ limit. For the threshold analysis, predicted probabilities were calculated across the observed range of daily fire hotspots, while air temperature and relative humidity were held constant at their respective mean values. The numbers of fire hotspots corresponding to estimated exceedance probabilities of 50% and 80% were then determined.

3 Results and discussion

Daily $PM_{2.5}$ and PM_{10} concentrations in Humaitá-AM showed clear seasonality over the years (Figure 2), controlled by wet removal during the rainy season and by the increase in emissions associated with fires in the dry season. The combination of high temperatures, low precipitation, reduced relative humidity, atmospheric stability, and weak ventilation favored the accumulation of pollutants near the surface, an atmospheric pattern similar to that found by Fujino and Miyamoto (2022) and Souza et al. (2025).

From June 2023, the decrease in precipitation contributed to high PM concentrations. During this period, mean $PM_{2.5}$ concentrations ranged from 12.3 to 16.3 μg m^{-3}, while PM_{10} reached a daily maximum of 68.4 μg m^{-3}. Subsequently, with the return of the rains in October, wet deposition processes promoted the gradual reduction of concentrations, as observed by Moura et al. (2024), who found a negative correlation between these variables.

In 2024, there was a marked increase in $PM_{2.5}$ and PM_{10} concentrations (Figures 2b and 2d), with an abrupt increase from August onward. The near absence of precipitation during this month, with only 5.4 mm accumulated, favored the accumulation of these aerosols in the lower levels of the atmosphere. Daily maximum $PM_{2.5}$ concentrations reached 143.8 μg m^{-3} in August and increased to 172.3 μg m^{-3} in September, while those of PM_{10} reached 148.2 and 176.0 μg m^{-3}, respectively.

The magnitude of this event shows that Humaitá, located close to the main emitting sources in the deforestation arc, is among the areas most affected by fire episodes, a condition that favored, in 2024, the formation of extensive smoke plumes transported hundreds of kilometers towards Southeast and Southern Brazil via the South American Low-Level Jet (SALLJ) (Forgioni et al., 2025).

The reduction in $PM_{2.5}$ and PM_{10} concentrations observed from October coincided with the reestablishment of the rainfall regime (Figure 3), with monthly precipitation increasing from 27.4 mm in September 2023 to 44.4 mm in October and 130.1 mm in November of the same year. In 2024, the pattern was similar: after a minimum of 5.4 mm in August, precipitation recovered to 43.3 mm in September and 83.4 mm in October, accompanied by an abrupt reduction in mean $PM_{2.5}$ concentrations from 55.7 μg m^{-3} in September to 9.5 μg m^{-3} in October.

Studies conducted in Campo Grande (Mato Grosso do Sul state) demonstrated that precipitation of up to 31.4 mm reduces PM concentrations through wet deposition. The capture of particles by raindrops (below-cloud scavenging) progressively removes accumulated aerosols, reducing the residence time of particles in the atmosphere (Fujino and Miyamoto, 2022; Souza et al., 2025).

The time series of hotspot counts (Table 1) shows a 31% increase in the number of fires between 2023 and 2024, with 74% of the hotspots recorded in 2024 concentrated in August and September. In that year, Humaitá ranked among the six municipalities with the highest number of active hotspots in Amazonas, accounting for approximately 5.5% of the state total recorded (INPE, 2024).

The drought recorded in the Amazon between 2023 and 2024, documented by Marengo et al. (2024), was one of the most severe ever observed, with water deficits that favored the vulnerability of vegetation to ignition and fire spread. Signori et al. (2026) demonstrated that climate variability modes, particularly El Niño, exerted a determining influence on the occurrence of fires in South America, a period in which Humaitá recorded accumulated precipitation of only 12.8 mm between June and August. These extreme climate events intensified the forest degradation caused by fires in 2024, with an increase of more than 400% relative to the reference years (Bourgoin et al., 2025).

The spatial distribution showed an increase in hotspots in the western portion of the municipality, especially along the BR-230 and BR-319 highways, as well as around the peripheral zones of the city (Figure 4). The opening and consolidation of these road axes act as vectors

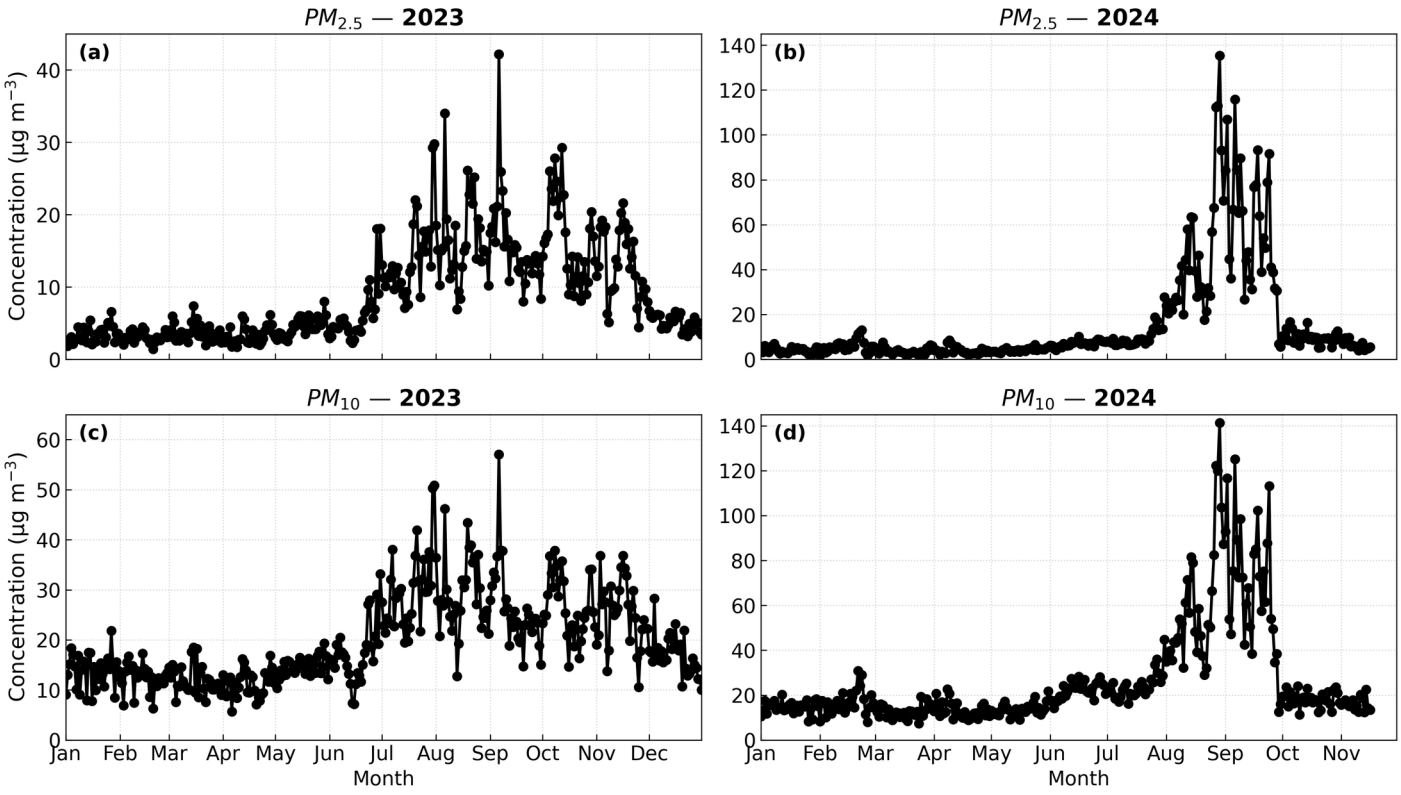


Figure 2. Daily $PM_{2.5}$ (a–b) and PM_{10} (c–d) concentrations over the months in Humaitá-AM in 2023 and 2024. Data obtained from the automatic atmospheric monitoring station (ECOPM).

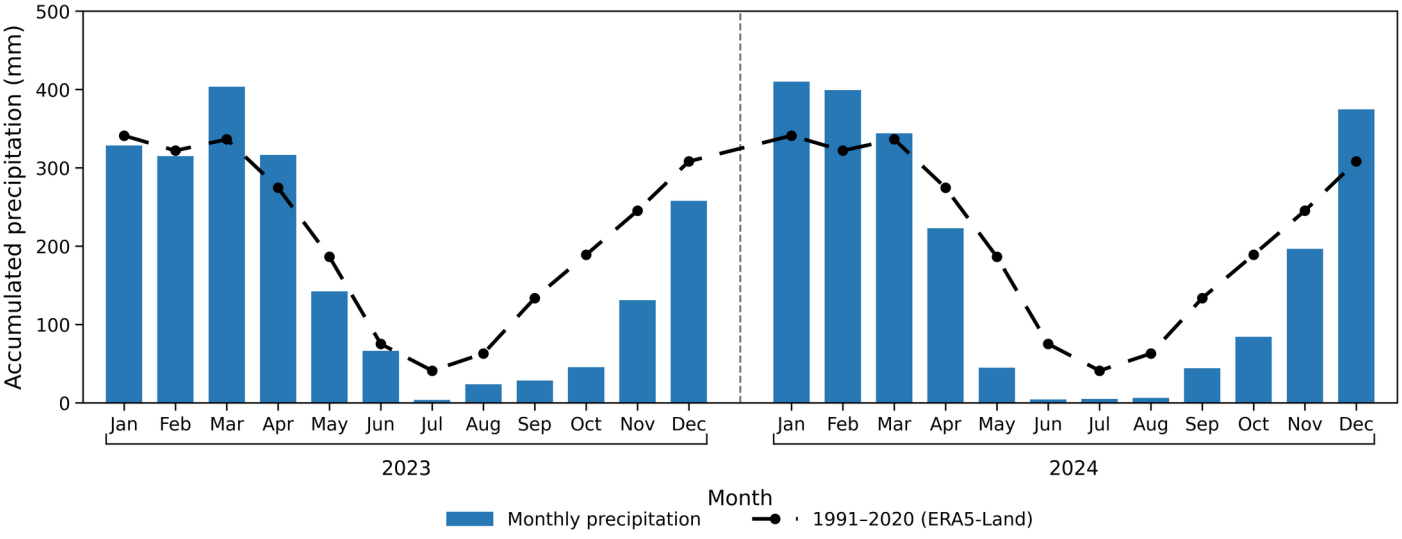


Figure 3. Monthly accumulated precipitation in Humaitá-AM during 2023 and 2024, obtained from ERA5-Land reanalysis data (ECMWF). The dashed line indicates the 1991-2020 monthly climatological mean.

Table 1. Monthly distribution of fire hotspots recorded in the municipality of Humaitá-AM in 2023 and 2024.

Year	Jan	Feb	Mar	Apr	May	Jun	Jul	Aug	Sep	Oct	Nov	Dec	Annual total
2023	1	1	0	1	1	2	56	331	533	114	31	9	1080
2024	6	1	2	0	2	14	261	679	370	67	12	1	1415

Source: Queimadas/INPE Program (2024).

of deforestation, forest fragmentation, and increased fire recurrence in municipalities within the deforestation arc (Santos et al., 2023).

Studies show that during the extreme events of 2010, 2016, and 2024, forest degradation exceeded deforestation by factors of 1.3, 1.7, and 4.2, respectively (Bourgoin et al., 2025), evidencing changes in forest degradation and fire dynamics in the Amazon (Ferreira et al., 2023). In this context, fires can contribute more than 80% of surface $PM_{2.5}$ concentrations during the dry season in the Amazon (Butt et al., 2020), affecting approximately 24 million Amazonian inhabitants (Urrutia-Pereira et al., 2021), indicating that the impacts of smoke extend beyond the areas directly affected by fire.

The predominance of northerly and northeasterly winds during the third quarter of 2023 and of southerly winds in 2024 (Figure 5) favored the regional transport of PM toward the monitoring point. However, the low wind speeds observed during the height of the dry season, predominantly between 0.8 and 1.6 m/s, reduced the local atmospheric dispersion capacity, favoring the accumulation of pollutants near the surface. Under weak wind conditions, mechanical turbulence becomes insufficient to promote the efficient dilution of pollutants in the atmosphere.

This effect is amplified during the nighttime, when radiative cooling, associated with weak wind conditions, suppresses convective processes and reduces the height of the nocturnal boundary layer (hn). Mendonça et al. (2025), in a study conducted in Central Amazonia with micrometeorological measurements from the Amazon Tall Tower Observatory (ATTO), demonstrated that the lowest hn values occur during the dry period associated with El Niño (~100 ± 27 m), while during the rainy period under the influence of La Niña the boundary layer height reaches approximately 270 ± 40 m. Under these conditions, the reduction in vertical mixing favors the accumulation of pollutants near the surface in the study area.

The monthly descriptive statistics (Table 2) revealed a seasonal pattern consistent with that observed in regions under the direct influence of fires in the Amazon. During the rainy season, $PM_{2.5}$ concentrations remained below 7 μg m^{-3}, with standard deviations below 4 μg m^{-3}, values close to the Amazonian atmospheric background of 1.5 μg m^{-3}, associated with the predominance of natural biogenic emissions during this period (Butt et al., 2020).

In the 2023 dry season, $PM_{2.5}$ means ranged between 12.3 μg m^{-3} (July) and 16.3 μg m^{-3} (October), with a daily maximum of up to 59.1 μg m^{-3}. In 2024, the statistical structure of the distributions changed, with averages of 43.1 ± 30.0 μg m^{-3} in August and 55.7 ± 34.8 μg m^{-3} in September, higher than those recorded in Porto Velho (RO) during intense fire episodes (36.3 ± 31.1 μg m^{-3}) (Jang and Jung, 2023), evidencing the severity of the event recorded in 2024. The daily maxima of 143.8 μg m^{-3} and 172.3 μg m^{-3} recorded in August and Septem-

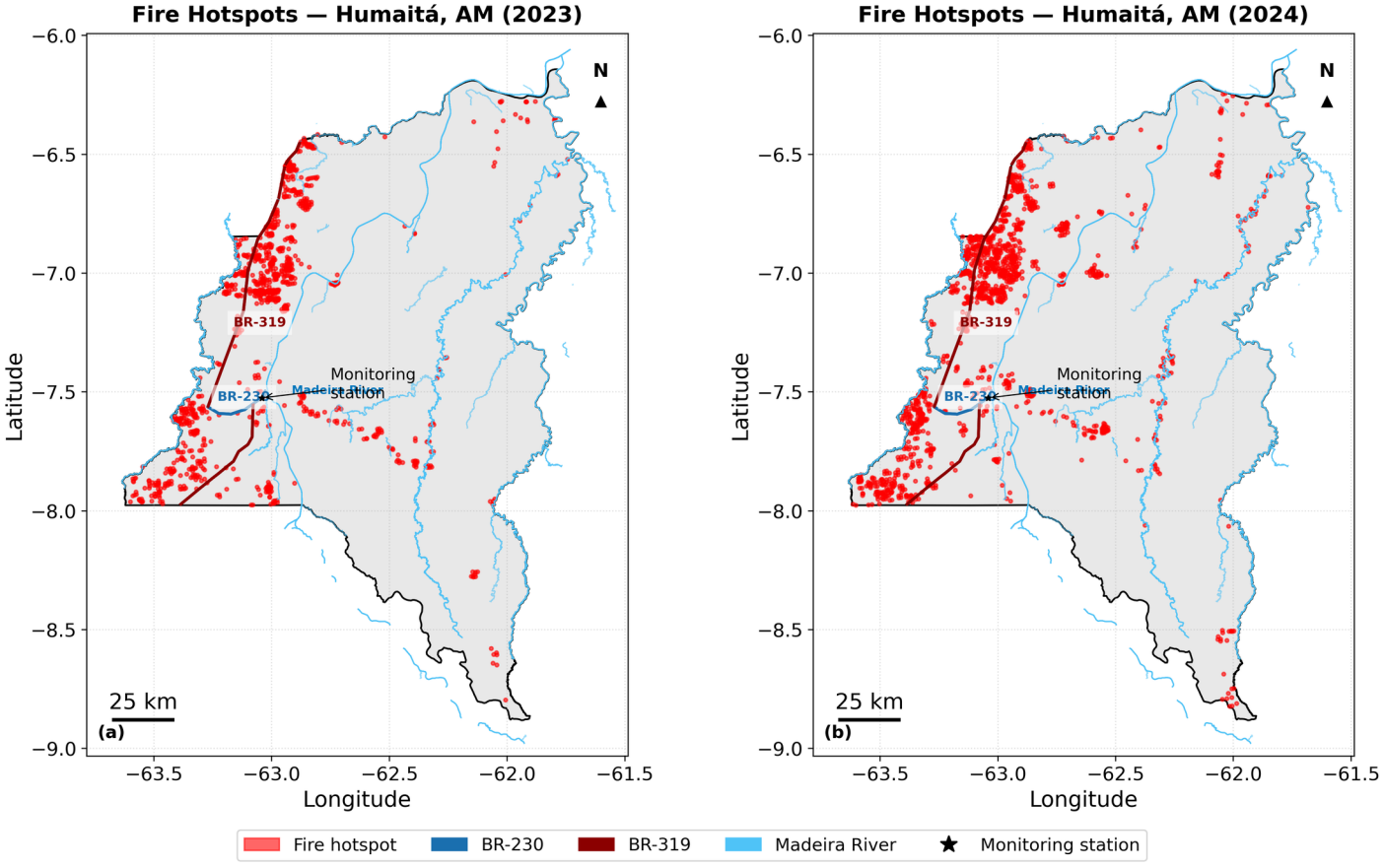


Figure 4. Spatial distribution of fire hotspots in Humaitá-AM in 2023 and 2024.
Notes: data from the Queimadas/INPE Program; red points represent fire hotspots.

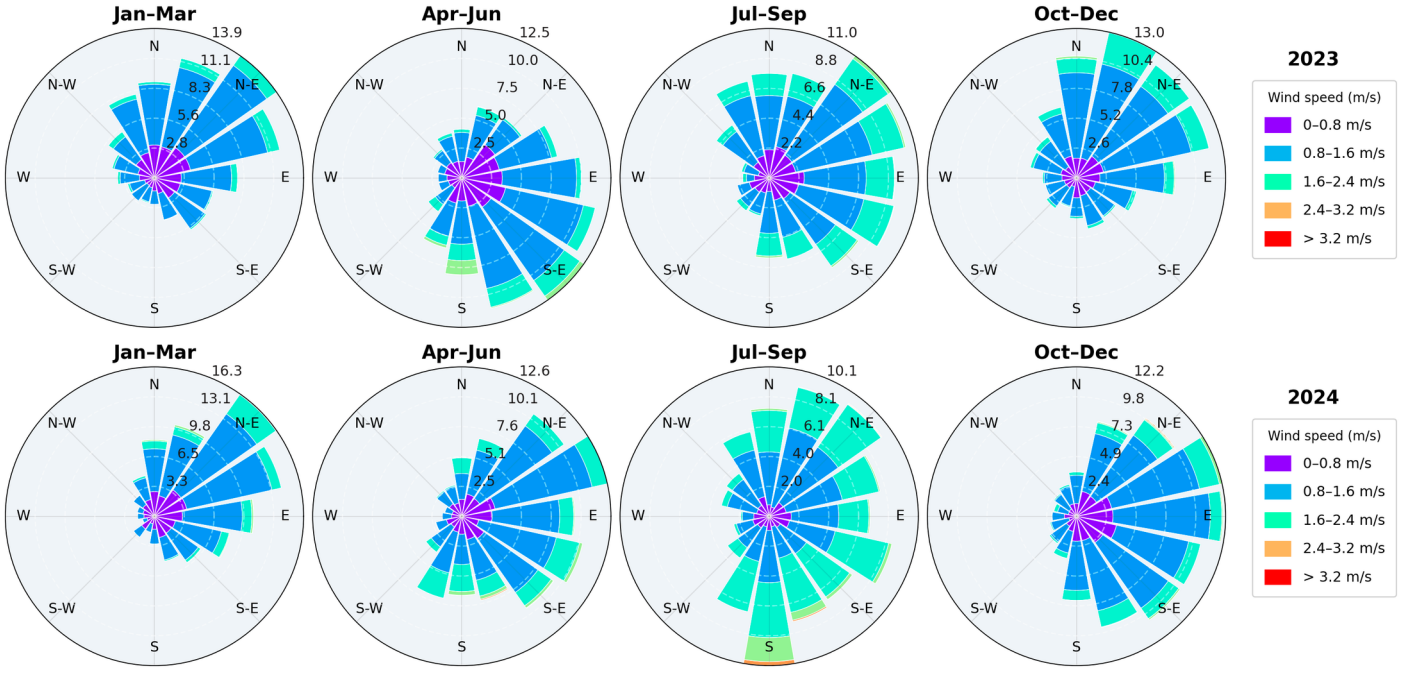


Figure 5. Quarterly wind roses for 2023 and 2024 in Humaitá-AM, showing the frequency (%) and intensity of wind speed by predominant direction

ber exceeded the values found for the Southwestern Amazon, where mean concentrations frequently exceed 33 μg m^{-3} and daily peaks approach 100 μg m^{-3} (Butt et al., 2020).

During the peak of the 2024 dry season, the $PM_{2.5}/PM_{10}$ ratio ranged between 0.76 and 0.84 in August and September, respectively, indicating the dominance of the fine fraction and confirming biomass burning as the main emitting source. A value close to 0.79 was reported for Santarém (PA) during the 2023 dry season, where biomass burning was identified as the dominant source, with 94% of exceedances occurring between July and December (Almeida et al., 2026). This predominance of the fine fraction contrasts with urban environments dominated by vehicular traffic, where the $PM_{2.5}/PM_{10}$ ratio typically ranges between 0.4 and 0.6, as reported for the Lima-Callao Metropolitan Area, Peru (Espinoza-Guillen et al., 2024), reinforcing that fires, rather than local vehicular emissions, constitute the dominant source of PM in Humaitá.

The positive skewness of the distributions indicates the occurrence of extreme peaks, a characteristic pattern of municipalities in the deforestation arc. For comparison, the $PM_{2.5}$ average in the São Paulo Metropolitan Region, one of the largest metropolises in the Southern Hemisphere, was 18.0 ± 12.5 μg m^{-3} (Vieira et al., 2023). The monthly averages in August and September 2024 were more than twice this value, evidencing that, during fires, a small Amazonian city of 57,000 inhabitants, without heavy industries, presented concentrations higher than those recorded in one of the country's largest metropolises.

From a toxicological standpoint, fine particles have a longer atmospheric residence time, on the order of days to weeks, with a greater long-distance transport capacity and a greater potential to penetrate the lower respiratory tract, reaching the lung alveoli and potentially crossing the epithelial barrier (Feng et al., 2024).

The Pearson correlations (Table 3) revealed that fire hotspots were the main predictor of $PM_{2.5}$ ($r = 0.777$; $p < 0.001$) and PM_{10} ($r = 0.785$; $p < 0.001$) concentrations, followed by relative humidity ($PM_{2.5}$: $r = -0.694$; PM_{10}: $r = -0.761$) and temperature ($PM_{2.5}$: $r = 0.592$; PM_{10}: $r = 0.617$), all significant at $p < 0.01$, while precipitation showed a moderate negative correlation with both pollutants ($PM_{2.5}$: $r = -0.493$, $p < 0.05$; PM_{10}: $r = -0.552$, $p < 0.01$). The coefficients of determination (R^2) indicate that approximately 60% of the monthly variability in $PM_{2.5}$ and PM_{10} concentrations was associated with fire activity, a result consistente with the findings of Butt et al. (2020), who estimated that fires contributed more than 80% of surface $PM_{2.5}$ concentrations during the dry season in the Amazon.

The negative correlations observed for relative humidity and precipitation reflect the role of wet deposition in aerosol removal, since the reduction of these variables decreases the efficiency of wet scavenging and prolongs the residence time of particles in the atmosphere. Temperature showed a positive correlation with both particulate fractions, reflecting the association between high temperatures, reduced precipitation, and intensified fires during the Amazonian dry season. The correlations obtained from monthly means predominantly reflect the seasonal behavior of the variables and do not imply direct causality.

The backward trajectory analyses (HYSPLIT) for August and September of 2023 and 2024 (Figure 6) provided physical evidence for understanding both the origin of the particles and the intensification of the observed concentrations. In 2023, the trajectories indicated the predominance of air masses from the North and Northeast,

Table 2. Monthly descriptive statistics of fine particulate matter ($PM_{2.5}$) and inhalable particulate matter (PM_{10}) concentrations in 2023 and 2024

Month	$PM_{2.5}$ – 2023							PM_{10} – 2023						
	Mean	SD	Min	P25	P50	P75	Max	Mean	SD	Min	P25	P50	P75	Max
Jan	3.4	2.1	0.6	1.9	2.9	4.4	17.8	13.5	7.6	1.8	7.2	12.3	18.4	36.5
Feb	3	1.6	0.4	2	2.8	3.6	14.2	12	6.5	1.1	6.8	10.6	16.9	32.8
Mar	3.7	1.9	0.9	2.3	3.3	4.6	11.6	11.5	5.4	2.4	7.4	10.6	14.9	27.1
Apr	3.2	1.9	0.6	1.9	2.7	3.8	16.1	10.9	5.6	1.4	6.4	10.1	14.2	27.7
May	4.5	2.3	1	3.2	4	5.2	19.9	14.2	5.8	3.3	10.1	13.2	17.8	31.8
Jun	5.1	2.9	1	3.4	4.3	5.9	22.6	15.6	6.9	2.4	10.5	14.3	19.2	35.7
Jul	12.3	8.8	3.6	6.1	9.1	15.1	59.1	27.1	12.7	9.9	17.5	23.2	33.6	68.4
Aug	15.1	7.6	3.8	9.3	13.3	18.6	48.4	26.6	11	4.5	18.9	23.8	32.6	61.9
Sep	15.1	6.5	2.7	11.3	13.4	17.9	46	24.6	9.1	5.5	18.6	22.6	29.5	51.9
Oct	16.3	7.6	4.7	10.5	14.9	20.7	50	26.1	9.8	8.3	18.5	24.7	31.7	55.9
Nov	12.7	5.7	2	8.4	12.1	16.6	31.7	24.1	9.8	3.1	17.2	22.5	30.3	52.4
Dec	5	2	1	3.6	4.7	6.1	14.3	16	6.5	2.8	11.4	14.6	20	36.2
Month	**$PM_{2.5}$ – 2024**							**PM_{10} – 2024**						
	Mean	SD	Min	P25	P50	P75	Max	Mean	SD	Min	P25	P50	P75	Max
Jan	4.1	1.9	0.6	2.7	3.8	5.2	13.1	14.3	6.3	1.4	9.4	13.9	17.9	32.7
Feb	5.6	3.4	0.4	3.2	4.7	7.1	16.1	16.2	7.5	1.6	10.4	14.8	20.9	38.2
Mar	3.5	1.9	0.6	2.3	3.1	4.6	17	12.3	5.8	1.7	7.8	11.7	15.9	29.2
Apr	3.8	2.2	0.7	2.3	3.1	4.7	14.2	12.7	5.7	2.5	8.4	12.1	16	30.7
May	4	1.5	1	3.1	3.8	4.7	16.1	12.9	4.6	3.5	9.7	12.4	15.2	27.6
Jun	6.6	3.3	2.7	4.4	5.7	8	32.6	20.8	8.8	8.9	14.3	18.2	25.4	51.3
Jul	8.9	3.9	3.1	6.3	7.5	10.2	29.7	22	7.2	7.2	17.2	20.7	25.5	47.6
Aug	43.1	30	7.9	21.5	32.2	56.1	143.8	56.6	31	11.3	32.2	47.5	73.6	148.2
Sep	55.7	34.8	1.8	28.5	47.4	79.2	172.3	66.1	35.4	2.7	37.6	60.9	90.2	176
Oct	9.5	4.1	2.1	6.9	8.9	10.9	27.9	17.6	6.2	4.4	13.5	16.7	21.2	35.8
Nov	6.5	2.6	1.4	4.9	6.3	7.9	15.8	15.2	5.8	3	11.5	14.8	18.6	30.9

Note: SD = standard deviation; Min = minimum value; P25 = 25th percentile; P50 = median; P75 = 75th percentile; Max = maximum value. Concentrations are expressed in μg m^{-3}.

Table 3. Pearson correlations (r), significance (p), and coefficient of determination (R^2) between $PM_{2.5}$, PM_{10}, fire hotspots, and meteorological variables (temperature, relative humidity, and precipitation) in 2023 and 2024 (n = 23)

Variable pair	Pearson r	R^2	p-value	n
$PM_{2.5}$ × Fire hotspots	0.777	0.604	1×10^{-5}	23
$PM_{2.5}$ × Temperature (°C)	0.592	0.350	2.94×10^{-3}	23
$PM_{2.5}$ × Relative humidity (%)	-0.694	0.481	2.40×10^{-4}	23
$PM_{2.5}$ × Precipitation	-0.493	0.243	1.69×10^{-2}	23
PM_{10} × Fire hotspots	0.785	0.616	1×10^{-5}	23
PM_{10} × Temperature (°C)	0.617	0.381	1.70×10^{-3}	23
PM_{10} × Relative humidity (%)	-0.761	0.580	2×10^{-5}	23
PM_{10} × Precipitation	-0.552	0.304	6.34×10^{-3}	23

at low altitudes (< 500 m above ground level), suggesting a predominantly regional and local contribution. The integration of continuous concentration monitoring with backward trajectory modeling allowed the episodes of highest concentration to be attributed not only to local emissions but also to the regional transport of aerosols, expanding the capacity to interpret the atmospheric processes associated with extreme pollution events.

The August and September 2024 trajectories showed a marked change in the transport pattern, indicating a growing contribution of air masses from the South and Southeast, originating from Rondônia and Mato Grosso and transported in the low atmospheric boundary layer (< 200 m), where concentrations are highest. This pattern is physically consistent with the South American Low-Level Jet (SALLJ) acting as a mechanism for transporting biomass aerosols from the Amazon to other regions, as demonstrated by Forgioni et al. (2025) for the extreme event of September 2024.

Prist et al. (2023) demonstrated that fine particles can disperse over distances greater than 500 km. In the present study, the September 2024 trajectories indicate that air masses traveled distances greater than 800 km before reaching Humaitá, corroborating the role of regional transport in amplifying local concentrations. A similar result was observed by Moura et al. (2024) in Amazonian cities of Mato

Grosso, where significant positive correlations between fire hotspots and $PM_{2.5}$ were recorded even in municipalities without significant local fire activity, evidencing the influence of regional and long-range transport of atmospheric aerosols.

The consistency among the transport patterns identified by HYSPLIT, the significant correlation between $PM_{2.5}$ and fire hotspots ($r = 0.777$; $p < 0.001$), and the values reported by Prist et al. (2023) and Moura et al. (2024) reinforces that, in years of severe drought, fire acts as the main modulator of PM concentrations in the Amazonian atmosphere, with impacts that transcend municipal and regional boundaries.

The critical threshold analysis revealed a dose–response relationship between fire hotspots and $PM_{2.5}$ concentrations (Figure 7). The Kruskal–Wallis test confirmed significant differences in the average $PM_{2.5}$ concentrations among the four fire intensity classes ($H = 252.1$; $p < 0.001$), evidencing that the increase in fire activity is associated with the progressive elevation of fine PM concentrations. On days without recorded hotspots (n = 490), the $PM_{2.5}$ average remained below 5 μg m^{-3}, indicating the contribution of other emitting sources. With increasing hotspot intensity, the averages shifted progressively: low class (1–5 hotspots, n = 99): ~12 μg m^{-3}; moderate (6–20 hotspots, n = 60): ~18 μg m^{-3}; and high (>20 hotspots, n = 37): ~28 μg m^{-3}, almost twice the daily limit of the CONAMA Resolution.

The multivariate binary logistic regression (hotspots + temperature + relative humidity) showed excellent discriminatory capacity (AUC-ROC = 0.89), indicating a high ability of the model to distinguish days of exceedance of the daily $PM_{2.5}$ limit of 15 μg m^{-3}. The odds ratios were 1.029 for fire hotspots, 1.407 for air temperature, and 0.821 for relative humidity, indicating positive associations of fire hotspots and temperature with the odds of exceedance and a negative association with relative humidity, while holding the other variables constant. Holding air temperature and relative humidity constant at their respective mean values, the operational thresholds derived from the model indicate that the predicted probability of exceedance reaches 50% with 85 hotspots/day and 80% with 134 hotspots/day recorded in the municipality. The identification of these thresholds represents a quantitative result of the statistical model, allowing the number of fire hotspots to be translated into estimated probabilities of exceeding the daily $PM_{2.5}$ limit.

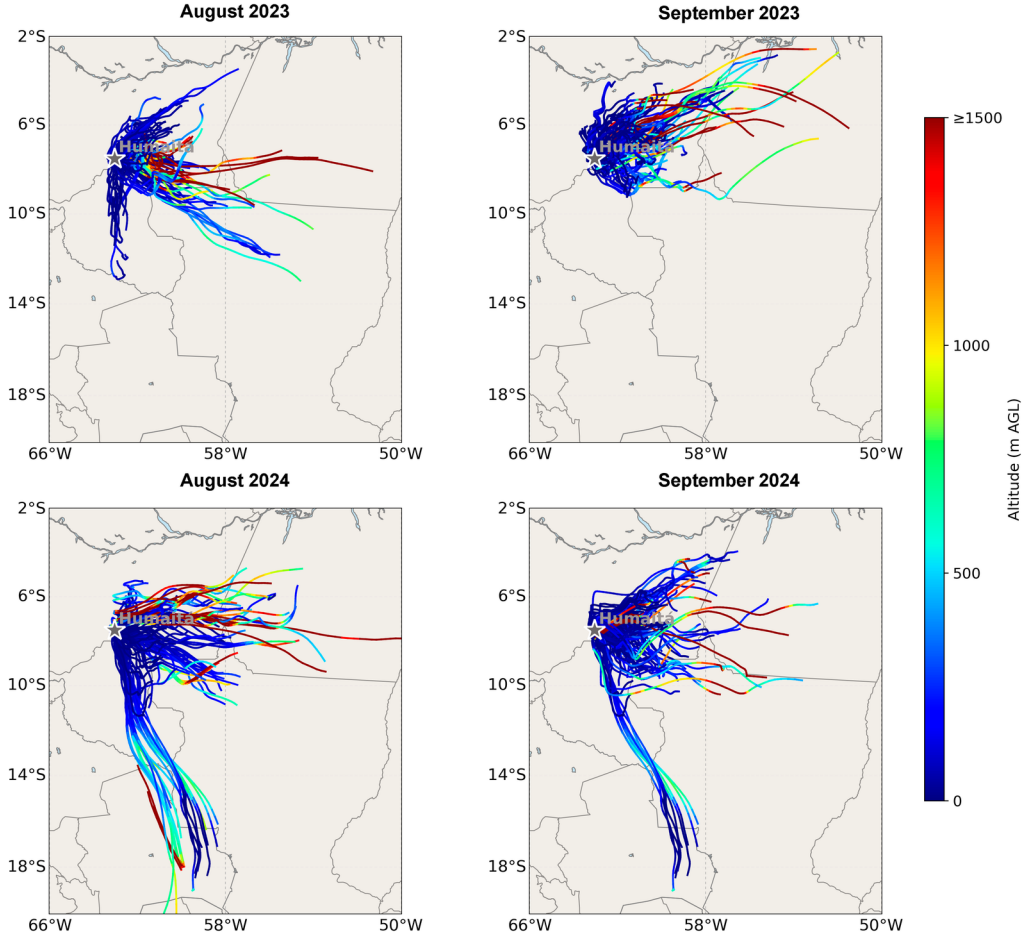


Figure 6. Backward air mass trajectories (72 h) from the HYSPLIT model (NOAA/GDAS, 1°) for August and September of 2023 and 2024 in Humaitá-AM. Colors indicate altitude (m AGL). Grey star: monitoring station.

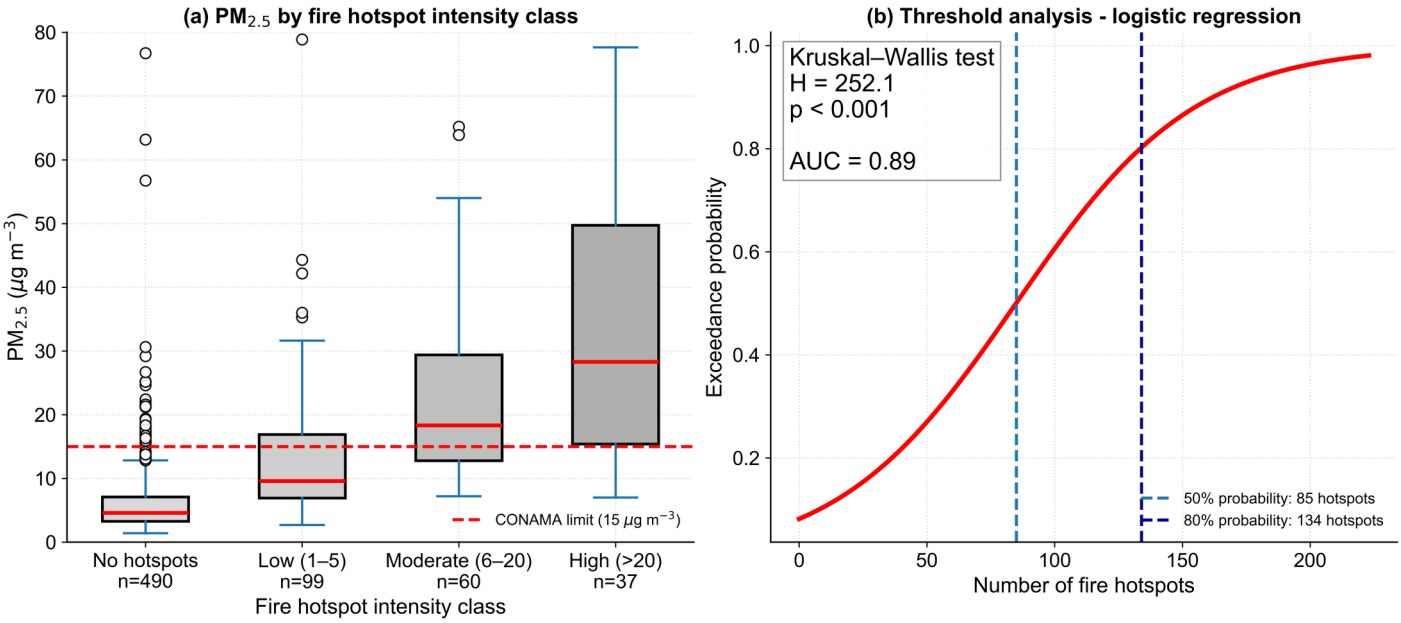


Figure 7. Relationship between fire hotspots and $PM_{2.5}$ concentrations in Humaitá-AM between 2023 and 2024. (a) Distribution of $PM_{2.5}$ concentrations by fire hotspot class. (b) Probability of exceeding the daily $PM_{2.5}$ limit of 15 μg m^{-3} estimated by multivariate logistic regression, with air temperature and relative humidity held constant at their respective mean values.

These values represent operational thresholds estimated for Humaitá and have potential application in air quality early warning systems. As the number of fire hotspots increases, the model indicates an increasing probability of exceeding the daily $PM_{2.5}$ limit of 15 μg m^{-3}.

Rincon et al. (2022) applied a logistic regression model in the Venezuelan context and obtained an overall success rate of 94% in classifying $PM_{2.5}$ exceedance days. Silva et al. (2020), in a dynamic wildfire warning system developed for the state of Acre, used the ROC curve to assess the performance of the fire risk model, demonstrating the applicability of this approach to warning systems. The methodological convergence among these studies supports the use of logistic regression as a tool for estimating the probability of $PM_{2.5}$ limit exceedance and indicates the potential applicability of probabilistic models in structuring early warning and air quality management systems based on continuous monitoring and fire data.

The classification of daily $PM_{2.5}$ averages according to the AQI of CONAMA Resolution No. 506/2024 (Figure 8) evidenced a marked contrast between the two analyzed years. In 2023, of the 183 monitored days during the period of fire influence (June–November), 37.2% presented concentrations above 15 μg m^{-3}, with a predominance of the Moderate category.

In 2024, the scenario was significantly more severe compared with 2023. Of the 123 monitored days during the months of July to October, 52.0% presented concentrations above the established daily limit of 15 μg m^{-3}, with a predominance of the Poor and Very Poor categories and the occurrence of episodes classified as Very Bad, reflecting the greater intensity and persistence of air quality degradation episodes.

The persistence of elevated $PM_{2.5}$ concentrations over the analyzed years evidences a scenario of recurrent exposure of the Humaitá population. In 2023 and 2024, 68 and 64 days above the daily limit were recorded, respectively. Although 2023 presented a higher number of exceedances, the episodes recorded in 2024 were more severe, characterized by persistently elevated concentrations.

Prolonged exposure to elevated $PM_{2.5}$ concentrations has important public health implications. Studies conducted in the Amazon demonstrate that PM from biomass burning is associated with inflammatory processes, DNA damage, and an increased risk of chronic diseases, including different types of cancer (Ellwanger et al., 2020). In the short term, intense smoke episodes are associated with an increased risk of acute myocardial infarction, heart failure, and the worsening of respiratory diseases within a few days after exposure (Yen and Chen, 2022).

In this context, the results observed in Humaitá indicate not only acute episodes of atmospheric pollution, but also a scenario of recurrent and prolonged exposure, potentially capable of increasing the respiratory and cardiovascular risks of the exposed local population, especially among children and the elderly. The World Health Organization (WHO) and CONAMA Resolution No. 506/2024 reinforce that there is no safe level of $PM_{2.5}$ exposure.

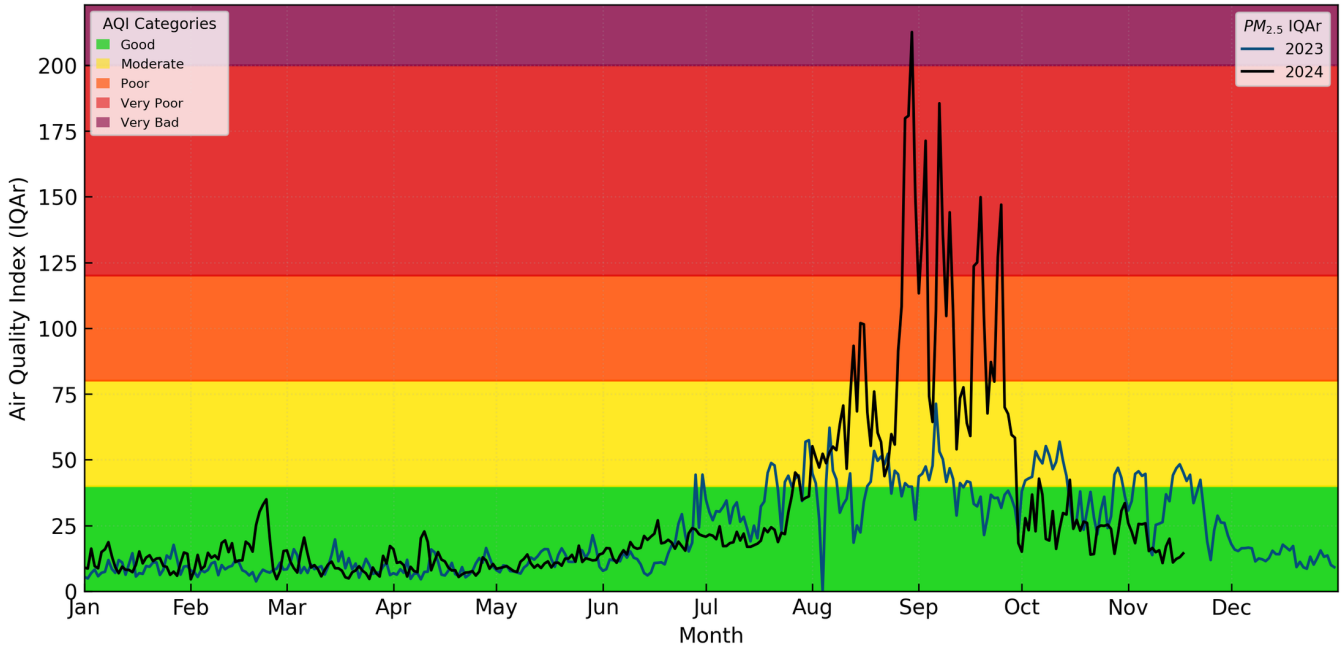


Figure 8. Daily classification of $PM_{2.5}$ concentrations according to the Air Quality Index (AQI) established by CONAMA Resolution No. 506/2024 in Humaitá, Amazonas, in 2023 and 2024.

4 Conclusion

The monitoring of PM concentrations in the urban area of Humaitá-AM evidenced strong seasonality, with reduced concentrations during the rainy season and a marked increase during the dry season, associated with the intensification of fires. In 2024, extreme episodes raised $PM_{2.5}$ and PM_{10} concentrations to levels higher than those recorded in important Brazilian urban centers, indicating severe air quality degradation in the Southern Amazon during critical fire events.

The comparison between 2023 and 2024 revealed greater severity of pollution episodes in 2024, with a higher occurrence of episodes classified in the "Very Poor" and "Very Bad" AQI categories. The backward trajectories obtained with the HYSPLIT model indicated the potential influence of regional aerosol transport from other areas of the Southern Amazon on the observed pollution episodes. Pearson correlations showed a strong association between fire hotspots and $PM_{2.5}$ and PM_{10} concentrations, supporting the important role of biomass burning in the seasonal variability of particulate matter. Meteorological conditions characterized by low relative humidity, absence of precipitation, and weak winds favored the accumulation of pollutants near the surface.

The integration of continuous air quality monitoring, atmospheric trajectory modeling, and statistical modeling based on logistic regression made it possible to advance beyond the descriptive characterization of pollution episodes, enabling a quantitative approach to understanding the influence of fires on air quality through the identification of thresholds associated with the increased probability of exceeding the standards established by Brazilian legislation.

The critical threshold analysis showed that, with air temperature and relative humidity held constant at their respective mean values, the predicted probability of exceeding the daily $PM_{2.5}$ limit of 15 μg m^{-3} reached 50% at 85 hotspots/day and 80% at 134 hotspots/day. These values represent quantitative operational thresholds estimated for Humaitá and may provide a basis for the development of air quality early warning approaches. Their application to other municipalities, however, requires local evaluation and validation considering regional meteorological and emission conditions.

The methodological procedures developed in this study constitute a basis for applications in other areas of the Amazon with limited monitoring infrastructure, with the potential to support the implementation of early warning systems, the planning of air quality management actions, and the improvement of environmental and health surveillance strategies.

Future studies should incorporate atmospheric modeling, chemical characterization of PM, and epidemiological indicators, expanding the understanding of the impacts of fires on air quality and public health in the Amazon.

5 Acknowledgments

The authors thank the Federal University of Amazonas (UFAM) and the Graduate Program in Environmental Sciences for providing the academic and scientific infrastructure required for the development of this study. The authors also acknowledge the Amazonas state Research Support Foundation (FAPEAM) for financial support through Public Call No. 003/2023 – PAINTER INFRA CT&I, and the Coordination for the Improvement of Higher Education Personnel (CAPES) for supporting academic training through the granting of a scholarship.

Authors' contributions

Carneiro, A.S.: Conceptualization, Data collection, Formal analysis, Data curation, Methodology, Investigation, Writing – original draft, Validation, Writing – review & editing; Menezes, J.A.: Conceptualization, Project administration, Data collection, Formal analysis, Data curation, Supervision, Resources, Software, Methodology, Investigation, Validation, Writing – review & editing; Pessoa, C.B.: Data collection, Data curation, Investigation, Validation, Visualization, Writing – review & editing; Castro, A.L.: Formal analysis, Methodology, Validation, Writing – review & editing; Palácios, R.S.: Formal analysis, Methodology, Validation, Writing – review & editing.

Conflicts of interest

The authors declare no conflicts of interest.

Funding

This study was supported by the Fundação de Amparo à Pesquisa do Estado do Amazonas (FAPEAM) through PAINTER INFRA CT&I Call No. 003/2023 and financed in part by the Coordenação de Aperfeiçoamento de Pessoal de Nível Superior – Brasil (CAPES) – Finance Code 001.

Declaration on the use of generative artificial intelligence

During the preparation of this manuscript, the authors used Claude Code (Anthropic) for language editing, grammar improvement, and manuscript organization. After using this tool, the author(s) reviewed and edited the content as necessary and take full responsibility for the content of the published article.

6 References

Almeida, D.O.; Santos Gomes, A.C.; Alves Batalha, S.S.; Mandú, T.B.; Souza do Nascimento, F.; Silva, G.V.; Costa, M.J.; Souza Fernandes Duarte, E., 2026. Spatiotemporal assessment of wildfire smoke exposure using a low-cost air quality monitoring system in a developing Amazonian city. Journal of Environmental Management, v. 401, 128875. https://doi.org/10.1016/j.jenvman.2026.128875.

Andreão, W.L.; Almeida Albuquerque, T.T., 2020. Fine particles as a public health indicator in Brazil: from monitoring to modeling. Air Quality, Atmosphere & Health, v. 13 (12), 1453-1463. https://doi.org/10.1007/s11869-020-00899-3

Bourgoin, C.; Beuchle, R.; Branco, A.; Carreiras, J.; Ceccherini, G.; Oom, D.; San-Miguel-Ayanz, J.; Sedano, F., 2025. Extensive fire-driven degradation in 2024 marks worst Amazon forest disturbance in over 2 decades. Biogeosciences, v. 22, 5247-5256. https://doi.org/10.5194/bg-22-5247-2025.

Brasil, 2020. Ministério do Meio Ambiente (MMA). Guia técnico para o monitoramento e avaliação da qualidade do ar. MMA, Brasília. https://www.gov.br/mma/pt-br/assuntos/meio-ambiente-urbano-recursos-hidricos-qualidade-ambiental/qualidade-do-ar/guia-tecnico-para-o-monitoramento-e-avaliacao-da-qualidade-do-ar.pdf

Butt, E.W.; Conibear, L.; Reddington, C.L.; Darbyshire, E.; Morgan, W.T.; Coe, H.; Artaxo, P.; Brito, J.; Knote, C.; Spracklen, D.V., 2020. Large air quality and human health impacts due to Amazon forest and vegetation fires. Environmental Research Communications, v. 2 (9), 095001. https://doi.org/10.1088/2515-7620/abb0db.

Conselho Nacional do Meio Ambiente (CONAMA), 2024. Resolução CONAMA nº 506, de 5 de julho de 2024. Diário Oficial da União, Brasília. https://conama.mma.gov.br.

Ellwanger, J.H.; Kulmann-Leal, B.; Kaminski, V.L.; Valverde-Villegas, J.M.; Veiga, A.B.G.; Spilki, F.R.; Fearnside, P.M.; Caesar, L.; Giatti, L.L.; Wallau, G.L.; Almeida, S.E.M.; Borba, M.R.; Hora, V.P.; Chies, J.A.B., 2020. Beyond diversity loss and climate change: impacts of Amazon deforestation on infectious diseases and public health. Anais da Academia Brasileira de Ciências, v. 92 (1), e20191375. https://doi.org/10.1590/0001-3765202020191375.

Espinoza-Guillen, J.A.; Alderete-Malpartida, M.B.; Navarro-Abarca, U.F.; Gómez-Muñoz, H.K., 2024. Temporal variation of the PM2.5/PM10 ratio and its association with meteorological factors in a South American megacity: Metropolitan Area of Lima-Callao, Peru. Environmental Monitoring and Assessment, v. 196 (5), 452. https://doi.org/10.1007/s10661-024-12611-4.

Fearnside, P.M., 2022. Desmatamento na Amazônia brasileira: história, índices e consequências. Editora do INPA, Manaus.

Feng, Y.; Castro, E.; Wei, Y.; Jin, T.; Qiu, X.; Dominici, F.; Schwartz, J., 2024. Long-term exposure to ambient PM2.5, particulate constituents and hospital admissions from non-respiratory infection. Nature Communications, v. 15 (1), 1518. https://doi.org/10.1038/s41467-024-45776-0.

Ferreira, I.J.M.; Campanharo, W.A.; Barbosa, M.L.F.; Silva, S.S.; Selaya, G.; Aragão, L.E.O.C.; Anderson, L.O., 2023. Assessment of fire hazard in Southwestern Amazon. Frontiers in Forests and Global Change, v. 6, 1107417. https://doi.org/10.3389/ffgc.2023.1107417.

Forgioni, F.P.; Bresciani, C.; Reis, A.; Müller, G.V.; Herdies, D.L.; Júnior, J.B.C.; Silva, F.D.S., 2025. Aerosol transport from Amazon biomass burning to Southern Brazil: a case study of an extreme event during September 2024. Atmosphere, v. 16 (10), 1138. https://doi.org/10.3390/atmos16101138.

Fujino, R.; Miyamoto, Y., 2022. PM2.5 decrease with precipitation as revealed by single-point ground-based observation. Atmospheric Science Letters, v. 23 (7), e1088. https://doi.org/10.1002/asl.1088.

Hersbach, H.; Bell, B.; Berrisford, P.; Hirahara, S.; Horányi, A.; Muñoz-Sabater, J. et al., 2020. The ERA5 global reanalysis. Quarterly Journal of the Royal Meteorological Society, v. 146 (730), 1999-2049. https://doi.org/10.1002/qj.3803.

Instituto Brasileiro de Geografia e Estatística (IBGE), 2022. Humaitá (AM): cidades e estados. https://www.ibge.gov.br/cidades-e-estados/am/humaita.html.

Instituto de Energia e Meio Ambiente (IEMA), 2024. Dimensionamento da rede básica de monitoramento da qualidade do ar no Brasil: cenários iniciais. IEMA, São Paulo. https://energiaeambiente.org.br/wp-content/uploads/2024/02/202402_dimensionamentoqarIEMA.pdf.

Instituto Nacional de Pesquisas Espaciais (INPE), 2024. Monitoramento dos focos ativos por estado, região ou bioma. Programa Queimadas. https://terrabrasilis.dpi.inpe.br/queimadas.

Jang, I.R.; Jung, S.I.; Lee, G.; Park, I.; Kim, S.B.; Kim, H.J., 2022. Quartz crystal microbalance with thermally-controlled surface adhesion for an efficient fine dust collection and sensing. Journal of Hazardous Materials, v. 424, 127560. https://doi.org/10.1016/j.jhazmat.2021.127560.

Jang, Y.-W.; Jung, G.-W., 2023. Temporal characteristics and sources of PM2.5 in Porto Velho of Amazon region in Brazil from 2020 to 2022. Sustainability, v. 15 (18), 14012. https://doi.org/10.3390/su151814012.

Jayaratne, R.; Liu, X.; Thai, P.; Dunbabin, M.; Morawska, L., 2018. The influence of humidity on the performance of a low-cost air particle mass sensor and the effect of atmospheric fog. Atmospheric Measurement Techniques, v. 11 (8), 4883-4890. https://doi.org/10.5194/amt-11-4883-2018.

Marengo, J.A.; Cunha, A.P.; Espinoza, J.-C.; Fu, R.; Schöngart, J.; Jimenez, J.C.; Costa, M.C.; Ribeiro, J.M.; Wongchuig, S.; Zhao, S., 2024. The drought of Amazonia in 2023-2024. American Journal of Climate Change, v. 13 (3), 567-597. https://doi.org/10.4236/ajcc.2024.133026.

Martins, P.A.S.; Querino, C.A.S.; Querino, J.K.A.S.; Moura, M.A.L.; Nunes, D.D.; Machado, N.G.; Biudes, M.S., 2023. Updating of the Köppen and Thornthwaite and Mather (1955) climate classification system for the Southern Amazonas. Revista do Departamento de Geografia, v. 43, e191137. https://doi.org/10.11606/eissn.2236-2878.rdg.2023.191137.

Mendonça, A.C.S.; Dias-Júnior, C.Q.; Acevedo, O.C.; Marra, D.M.; Cely-Toro, I.M.; Fisch, G. et al., 2025. Estimation of the nocturnal boundary layer height over the Central Amazon forest using turbulence measurements. Agricultural and Forest Meteorology, v. 367, 110469. https://doi.org/10.1016/j.agrformet.2025.110469.

Moura, F.R.; Machado, P.D.W.; Ramires, P.F.; Tavella, R.A.; Carvalho, H.; Silva Júnior, F.M.R., 2024. In the line of fire: analyzing burning impacts on air pollution and air quality in an Amazonian city, Brazil. Atmospheric Pollution Research, v. 15 (4), 102033. https://doi.org/10.1016/j.apr.2023.102033.

Pacheco, M.T.; Parmigiani, M.M.M.; Andrade, M.F.; Morawska, L.; Kumar, P., 2017. A review of emissions and concentrations of particulate matter in the three major metropolitan areas of Brazil. Journal of Transport & Health, v. 4, 53-72. https://doi.org/10.1016/j.jth.2017.01.008.

Palmisani, J.; Di Gilio, A.; Viana, M.; Gennaro, G.; Ferro, A., 2021. Indoor air quality evaluation in oncology units at two European hospitals: low-cost sensors for TVOCs, PM2.5 and CO2 real-time monitoring. Building and Environment, v. 205, 108237. https://doi.org/10.1016/j.buildenv.2021.108237.

Pereira, G.M.; Kamigauti, L.Y.; Pereira, R.F.; Santos, D.M.; Santos, T.S.; Martins, J.V. et al., 2025. Source apportionment and ecotoxicity of PM2.5 pollution events in a major Southern Hemisphere megacity: influence of a biofuel-impacted fleet and biomass burning. Atmospheric Chemistry and Physics, v. 25 (8), 4587-4616. https://doi.org/10.5194/acp-25-4587-2025.

Pereira, R.M.; Querino, J.K.A.S., 2025. Climatologia e conforto térmico no espaço urbano: um estudo de caso do município de Humaitá-AM, entre 2016 a 2020. Revista Brasileira de Climatologia, v. 36, 663-678. https://doi.org/10.55761/abclima.v36i21.18286.

Prist, P.R.; Sangermano, F.; Bailey, A.; Bugni, V.; Villalobos-Segura, M.C.; Pimiento-Quiroga, N.; Daszak, P.; Zambrana-Torrelio, C., 2023. Protecting Brazilian Amazon Indigenous territories reduces atmospheric particulates and avoids associated health impacts and costs. Communications Earth & Environment, v. 4 (1), 34. https://doi.org/10.1038/s43247-023-00704-w.

Rincon, G.; Morantes Quintana, G.; Gonzalez, A.; Buitrago, Y.; Gonzalez, J.C.; Molina, C.; Jones, B., 2022. $PM_{2.5}$ exceedances and source appointment as inputs for an early warning system. Environmental Geochemistry and Health, v. 44 (12), 4569-4593. https://doi.org/10.1007/s10653-021-01189-2.

Santos, J.L.; Yanai, A.M.; Graça, P.M.L.A.; Correia, F.W.S.; Fearnside, P.M., 2023. Amazon deforestation: simulated impact of Brazil's proposed BR-319 highway project. Environmental Monitoring and Assessment, v. 195, 1217. https://doi.org/10.1007/s10661-023-11820-7.

Santos, U.P.; Arbex, M.A.; Braga, A.L.F.; Mizutani, R.F.; Cançado, J.E.D.; Terra-Filho, M.; Chatkin, J.M., 2021. Environmental air pollution: respiratory effects. Jornal Brasileiro de Pneumologia, v. 47 (1), e20200267. https://doi.org/10.36416/1806-3756/e20200267.

Signori, R.T.; Mamani, L.; Cevalho, W.; Souza, I.P.; Kayano, M.T.; Oliveira, M.B.L.; Céron, W.L.; Andreoli, R.V.; Souza, R.A.F., 2026. How climate variability modes influenced the fires in South America during the extreme droughts of 2023-2024. Science of the Total Environment, v. 1028, 181705. https://doi.org/10.1016/j.scitotenv.2026.181705.

Silva, I.D.B.; Valle, M.E.; Barros, L.C.; Meyer, J.F.C.A., 2020. A wildfire warning system applied to the state of Acre in the Brazilian Amazon. Applied Soft Computing, v. 89, 106075. https://doi.org/10.1016/j.asoc.2020.106075.

Souza, A.; Oliveira-Júnior, J.F.; Cardoso, K.R.A.; Fernandes, W.A.; Pavao, H.G., 2025. The impact of meteorological variables on particulate matter concentrations. Atmosphere, v. 16 (7), 875. https://doi.org/10.3390/atmos16070875.

Stein, A.F.; Draxler, R.R.; Rolph, G.D.; Stunder, B.J.B.; Cohen, M.D.; Ngan, F., 2015. NOAA's HYSPLIT atmospheric transport and dispersion modeling system. Bulletin of the American Meteorological Society, v. 96 (12), 2059-2077. https://doi.org/10.1175/bams-d-14-00110.1.

United States Environmental Protection Agency (EPA), 2017. Air monitoring methods – criteria pollutants. Ambient Monitoring Technology Information Center (AMTIC). https://www.epa.gov/amtic.

United States Environmental Protection Agency (EPA), 2022. The enhanced air sensor guidebook. EPA/600/R-22/213. Office of Research and Development, Center for Environmental Measurement and Modeling. https://www.epa.gov/air-sensor-toolbox/how-use-air-sensors-air-sensor-guidebook.

Urrutia-Pereira, M.; Rizzo, L.V.; Chong-Neto, H.J.; Solé, D., 2021. Impact of exposure to smoke from biomass burning in the Amazon rain forest on human health. Jornal Brasileiro de Pneumologia, v. 47 (5), e20210219. https://doi.org/10.36416/1806-3756/e20210219.

Vieira, E.V.R.; Rosario, N.E.; Yamasoe, M.A.; Morais, F.G.; Martinez, P.J.P.; Landulfo, E.; Miranda, R.M., 2023. Chemical characterization and optical properties of the aerosol in São Paulo, Brazil. Atmosphere, v. 14 (9), 1460. https://doi.org/10.3390/atmos14091460.

Vormittag, E.M.P.A.A.; Cirqueira, S.S.R.; Neto, H.W.; Saldiva, P.H., 2021. Análise do monitoramento da qualidade do ar no Brasil. Estudos Avançados, v. 35 (102), 7-30. https://doi.org/10.1590/s0103-4014.2021.35102.002

World Health Organization (WHO), 2021. WHO global air quality guidelines: particulate matter (PM2.5 and PM10), ozone, nitrogen dioxide, sulfur dioxide and carbon monoxide. WHO, Geneva, 360 p.

Yamagishi, N.; Yamaguchi, T.; Kuga, T.; Taniguchi, M.; Khan, M.S.; Matsumoto, T.; Deguchi, Y.; Nagaoka, H.; Wakabayashi, K.; Watanabe, T., 2020. Development of a system for the detection of the inflammatory response induced by airborne fine particulate matter in rat tracheal epithelial cells. Toxicology Reports, v. 7, 900-908. https://doi.org/10.1016/j.toxrep.2020.06.011.

Yen, C.C.; Chen, P.L., 2022. Effect of short-term exposure to fine particulate matter and particulate matter pollutants on triggering acute myocardial infarction and acute heart failure. The American Journal of Cardiology, v. 175, 158-163. https://doi.org/10.1016/j.amjcard.2022.03.062.